Avalanches and bursts in low-pressure helium gas below the breakdown voltage

Z. Donkó
Research Institute for Solid State Physics of the Hungarian Academy of Sciences, P.O. B. 49, H-1525 Budapest, Hungary
(Received 24 October 1994; revised manuscript received 10 January 1995)

External ionizing particles may induce *electron avalanches* and *bursts* (sequences of avalanches) in a gas subjected to an electric field. The properties of these avalanches and bursts at a given pressure depend on the strength of the electric field, which in our case is considered to be homogeneous between two plane-parallel metal electrodes. With increasing voltage (V) applied to the electrodes the system may reach a state when the avalanches sustain themselves via ionization and secondary electron emission processes. We have found that this is a *critical state* that corresponds to a phase transition when the gas turns from an insulating state into a conducting state. Our computer simulations have shown that at the critical voltage ($V=V_c$) the $N(A)$ distribution of the number of electron avalanches forming a burst A and the $N(B)$ distribution of the total number of electrons participating in a burst B obey power laws $N(A) \propto A^{-\alpha}$ and $N(B) \propto B^{-\beta}$. The average values of A and B as functions of the voltage V also exhibit a power law dependence $\langle A \rangle \propto \tau^{-\delta}$ and $\langle B \rangle \propto \tau^{-\mu}$, where $\tau=(V_c-V)/V_c$. The nontrivial critical exponents α, β, δ, and μ were determined to an accuracy of a few percent.

PACS number(s): 05.40.+j, 05.70.Jk, 51.50.+v

I. INTRODUCTION

In the past few years considerable attention has been devoted to the study of avalanches in different types of dynamical systems [1–4]. Under appropriate conditions similar avalanches may occur in gases when external particles create charged particles (electron-ion pairs). The electrons created this way are accelerated if an electric field is applied and may create new electron-ion pairs in ionization processes. This phenomenon occurring in gases is called an *electron avalanche*. Electron avalanches play an important role in radiation detectors (proportional counters and Geiger-Müller tubes) [5] and in the breakdown process of gas discharges [6].

In our model we consider two parallel-plane metal electrodes separated by a distance of $L=1$ cm. Helium is used as the buffer gas. Only two types of charged particles, namely, electrons and He^+ ions, are considered. Low-energy electrons are injected into the gas as external particles. The injected electrons have a uniform spatial distribution between the electrodes.

The development of an electron avalanche can be traced in Fig. 1. The incoming particle (low-energy electron) entering the volume filled with the buffer gas forms an electron-ion pair. Under the influence of the electric field these particles (and the injected electron too) start to move towards the opposite biased electrodes. The electrons are considerably accelerated in the electric field and ionize He atoms thus creating additional electrons and positive ions. In this way the electrons are multiplicated and an electron avalanche builds up (which we call the *primary* avalanche). The *size* of an electron avalanche is characterized by the number of electrons involved. This number is usually called *multiplication* [7] and is denoted by M.

The motion of positive ions in the background gas is limited by collision processes (mainly symmetric charge transfer collisions) in which the number of ions does not change (unlike the number of electrons in electron impact ionization processes). If we neglect the electron-ion recombination in the gas phase (which is negligible under the conditions investigated) then the number of ions arriving at the cathode surface is equal to the number of ions created in the given avalanche. As the positive ions are able to liberate electrons from the cathode, additional electron avalanches may start (see Fig. 1). To distinguish these avalanches from avalanches initiated by external particles, we call them *secondary* avalanches. In this way

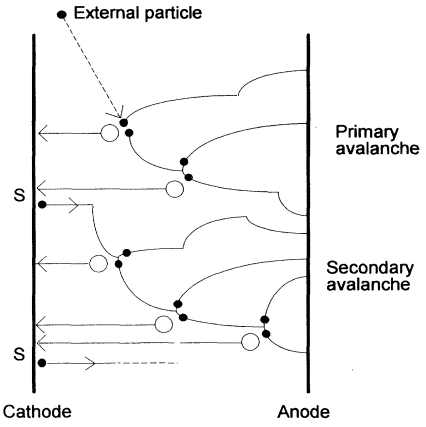

FIG. 1. Formation of electron avalanches and bursts. The external particle (low-energy electron) initiates a primary electron avalanche, which is followed by secondary avalanches. The splitting of the paths corresponds to ionizations; the changing direction of electron trajectories indicates elastic collisions and excitation collisions. S refers to secondary electron emission from the cathode. The solid circles correspond to electrons after their emission from the cathode and after ionizations; the open circles represent He^+ ions created in ionizing collisions.

one external particle may initiate several electron avalanches which together construct a *burst*. The number of electron avalanches in a burst is denoted by A and the size of a burst B is defined as the total number of electrons participating in the burst.

We suppose that the ion impact is the dominant process in secondary electron emission from the cathode. With increasing voltage the system may arrive at a state when the ionization and secondary electron emission processes become self-sustaining. This takes place at a certain voltage V_c when the average number of He^+ ions ($\langle M-1 \rangle$) created in (secondary) electron avalanches is just enough to liberate a "new" electron from the cathode:

$$\langle M(V_c)-1 \rangle \gamma = 1 , \quad (1)$$

where γ is the secondary electron emission coefficient (which can be viewed as the probability that an electron is emitted from the cathode due to the impact of a He^+ ion). In Eq. (1) we made use of the fact that the multiplication M at given pressure depends on the voltage applied to the electrodes.

We have found that at $V=V_c$ the system is in a *critical state* where the number of electron avalanches forming a burst A and the total number of electrons participating in a burst B have *self-similar, power-law distributions* $N(A) \propto A^{-\alpha}$ and $N(B) \propto B^{-\beta}$. In the vicinity of the critical state also the average values of A and B on the parameter $\tau=(V_c-V)/V_c$ featured a power-law dependence $\langle A \rangle \propto \tau^{-\delta}$ and $\langle B \rangle \propto \tau^{-\mu}$. The critical voltage of the system V_c, the $N(A)$ and $N(B)$ distributions, the $\langle A \rangle = f(\tau)$ and $\langle B \rangle = g(\tau)$ functions, and the α, β, δ, and μ critical exponents were determined from computer simulation of electron motion in a gas.

It is noted that our simple model is valid only in the voltage range $V \leq V_c$. The breakdown of the gas, which may occur at $V > V_c$, is beyond the scope of our investigations. The complicated phenomenon of breakdown can only be understood by considering a high number of elementary processes and active species, the effect of temporally overlapping avalanches, space charge formation, streamer formation, contribution of metastables and photons, etc. [6,8–14].

II. METHOD OF SIMULATION

To trace the trajectories of electrons in the gas the method of Monte Carlo (MC) simulation was chosen, which is widely used to describe particle transport in gases [15–19]. This method provides a fully kinetic description of the electrons' motion. Using a MC simulation, information about the behavior of individual particles is readily obtained. In the simulation the electrons move in a three-dimensional phase space, where their position is given by x, the position along the X axis perpendicular to the electrodes; v_X, the component of the velocity vector parallel to the X axis, and v_r, the component of the velocity vector to perpendicular to the X axis.

The position of an electron in phase space is completely defined by these three parameters as all radial directions are equivalent and we consider infinite electrodes in the simulation (i.e., we neglect edge effects). The kinetic energy ε and the angle between the velocity vector and X axis θ can alternatively be used instead of the v_X and v_r parameters [16]. The details of the principles of simulation are not given here; they may be found in detail in Refs. [15–18].

In the simulation the trajectories of single electrons are traced. The electrons moving in the gas may participate in different collision processes. The elementary processes considered in our model are anisotropic elastic scattering of electrons from He atoms, electron impact excitation, and ionization of He atoms. The applied MC procedure takes into account the accelerating effect of the electric field and the energy dependence of cross sections of the collision process (see Fig. 2). The positions of collisions are calculated in a random manner (taking into account the statistical properties of the particles' motion). The type of collision process actually occurring after a free path is also chosen randomly considering the cross sections of the possible elementary processes at the actual electron energy [16]. The total cross section of elementary processes are taken from [20,21]. The elastic scattering of electrons from He atoms is supposed to be anisotropic. The scattering angle of electrons is calculated randomly considering a formula fitted to differential cross section data [22,16]. The energy loss of electrons in elastic collisions is neglected. In the case of electron impact excitation no energy levels of the atom are distinguished and the electron may lose a randomly chosen energy between the first excited level and the ionization potential. The scattering of electrons in excitation processes is assumed to be isotropic. In ionizing collisions the trajectories of the incoming, scattered, and ejected electrons lie in the same plane. The share of remaining kinetic energy between the scattered and ejected electrons is assigned randomly.

The electrons are traced until they are absorbed by the (perfectly absorbing) anode electrode. The initial param-

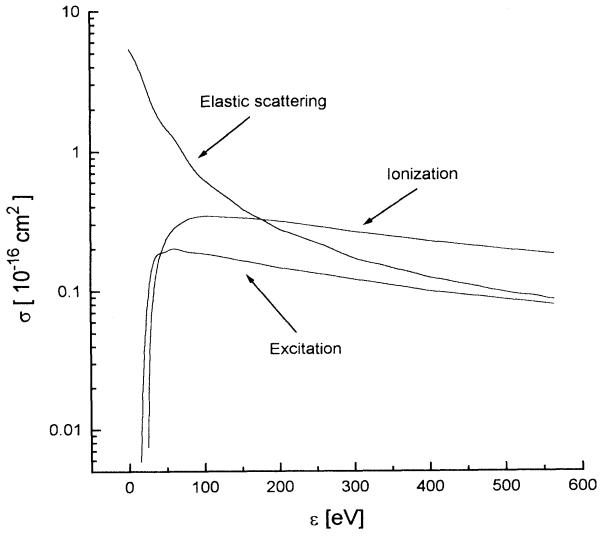

FIG. 2. Total cross sections of elementary electron collision processes considered in the model (helium).

eters (x,ε,θ) of additional electrons created in ionization processes are memorized (they are put in a list of electrons to be traced in the simulation program). The subsequent tracing of the trajectories of these electrons make it possible to simulate electron avalanches.

To model the formation of bursts we include in the simulation the emission of electrons from the cathode due to ion impact. To do this whenever an ionization process occurs, we put an electron at $x=0$ (cathode position) with a probability of $P=\gamma$ to the list of electrons to be traced. We start to simulate the new avalanche when the simulation of the current one has been completed.

III. RESULTS OF THE MODEL

To obtain the critical voltage V_c at a given gas pressure and secondary electron emission coefficient the average number of He^+ ions ($\langle M-1\rangle$) created in (secondary) electron avalanches was calculated as a function of voltage V. The results are shown in Fig. 3 for different values of the gas pressure p and for $\gamma=0.1$ secondary electron emission coefficient. It can be seen in Fig. 3 that (in the frame of our simple model) at 2 mbar pressure the average number of ions is insufficient to reach the critical state. At higher values of He pressure ($p=3-5$ mbar) there exists a critical voltage for each pressure value. At the given γ the critical voltage decreases with increasing pressure in the range of pressures investigated.

In the following we consider the case of $p=3$ mbar and $\gamma=0.1$. The results for different p-γ combinations are quite similar to those presented for $p=3$ mbar and $\gamma=0.1$.

The number of electrons participating in single avalanches M has a statistical distribution $N(M)$, which gives the number of avalanches with given M. The $N(M)$ distribution for $p=3$ mbar, $\gamma=0.1$ at the corresponding critical voltage $V_c=438$ V is plotted in Fig. 4 for primary and secondary electron avalanches. The plot of $N(M)$ shows that there is a high number of electron avalanches with $M=1$, when the incoming external electron or the electron emitted from the cathode reaches the anode without making any ionization. Both distributions plotted in Fig. 4 are quite broad; at high values of M they have a nearly exponential falloff.

The bursts consist of a different number of avalanches. The $N(A)$ distribution of the number of avalanches in a burst A is plotted in Fig. 5 for $p=3$ mbar, $\gamma=0.1$ at the critical voltage $V_c=438$ V. The data shown in Fig. 5 were obtained from the simulation of 5×10^5 bursts. It can be seen in Fig. 5 that $N(A)$ can be well approximated with a power-law function of A (except for the few smallest values of A)

$$N(A)\propto A^{-\alpha}. \tag{2}$$

The best-fitting exponent for Eq. (2) was found to be $\alpha=1.58$. Five simulation each consisting of 10^5 bursts have been carried out to obtain information about the accuracy of the exponent α. The exponent was determined from the range of $A=4-70$. The standard deviation of the resulting exponents was found to be $\sigma_\alpha=0.012$. Therefore the accuracy of the slope plotted in Fig. 5 is estimated to be $3\sigma_\alpha/\sqrt{5}\cong0.02$ (3 times the standard deviation).

The burst size distribution $N(B)$ for $p=3$ mbar, $\gamma=0.1$ at the critical voltage $V_c=438$ V is plotted in Fig. 6 for the burst size range $B=1-100$. It can be seen in Fig. 6 that $N(B)$ exhibits a characteristic power-law dependence on B

$$N(B)\propto B^{-\beta}. \tag{3}$$

The data shown in Fig. 6 were obtained from the simu-

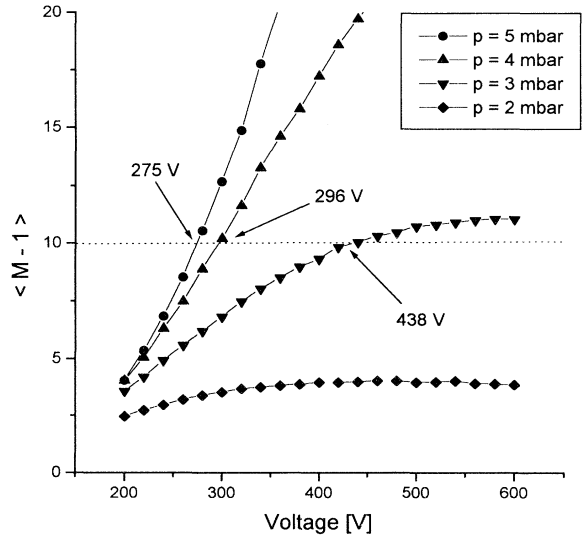

FIG. 3. Average number of He^+ ions ($\langle M-1\rangle$) created in (secondary) electron avalanches as a function of voltage V. The critical voltage values at different pressures for $\gamma=0.1$ secondary electron emission coefficient are indicated. Each data point is a result of simulation of 5×10^4 electron avalanches.

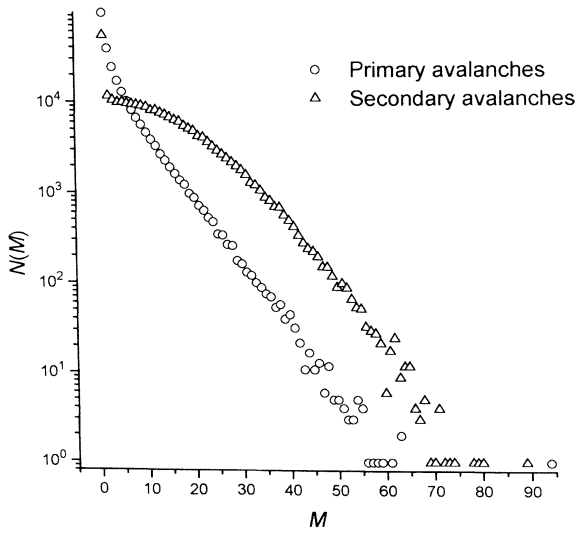

FIG. 4. $N(M)$ distribution of the multiplication M for $p=3$ mbar, $\gamma=0.1$ at the critical voltage $V_c=438$ V. The distributions were obtained from the simulation of 2.5×10^5 primary and secondary electron avalanches.

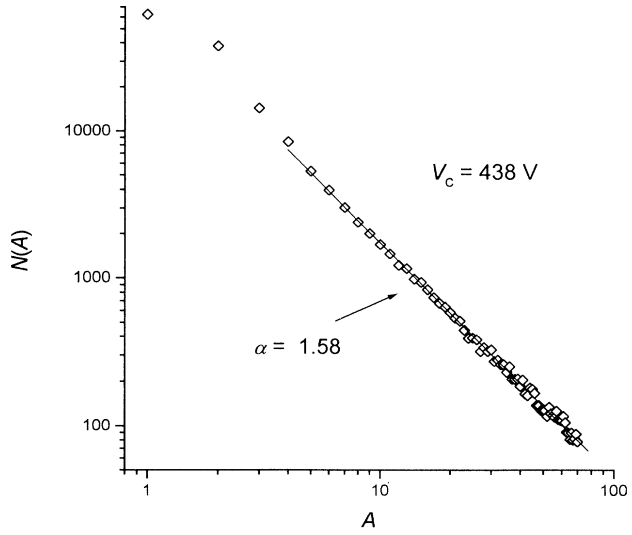

FIG. 5. $N(A)$ distribution of the number of avalanches (A) in a burst for $p=3$ mbar, $\gamma=0.1$ at the critical voltage $V_c=438$ V. The data were obtained from the simulation of 5×10^5 bursts. The $N(A)$ distribution can be well approximated by $N(A)\propto A^{-\alpha}$ with the critical exponent $\alpha=1.58$.

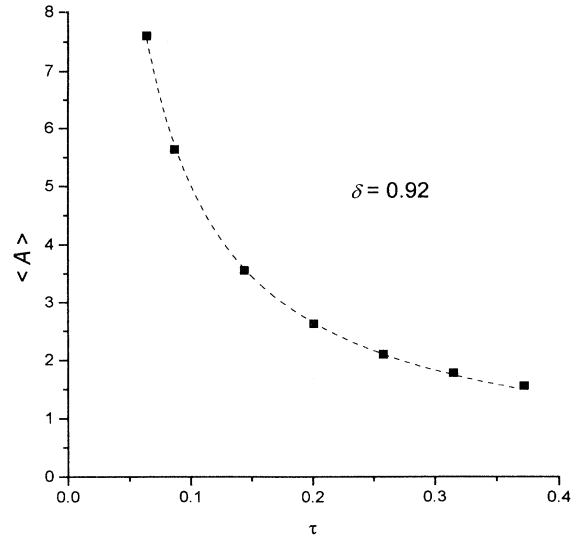

FIG. 7. Average number of avalanches constructing a burst ($\langle A\rangle$) as a function of the parameter $\tau=(V_c-V)/V_c$. The best-fitting critical exponent was found to be $\delta=0.92$. Each data point represents 10^6 simulated bursts.

lation of 10^6 bursts. The exponent in Eq. (3) was found to be $\beta=1.57$. In order to gain information about the accuracy of the exponent ten simulations each including 10^5 bursts have been carried out. The standard deviation of exponents determined this way was $\sigma_\beta=0.0083$ for 10^5 bursts. This means that the estimated accuracy (3 times the standard deviation) of the β exponent obtained from Fig. 6 is about 0.03. The inset in Fig. 6 shows the $N(B)$ distribution (obtained from the simulation of 5×10^5 bursts) for the burst size range $B=1-1000$.

The self-similar distributions presented in Figs. 5 and 6 indicate that *at the critical voltage there is no characteristic number of avalanches in a burst A and the burst size B.* This means that bursts of infinite length may also appear in the simulation resulting run time error of the program. To avoid this, bursts consisting of a limited number of avalanches and of a maximal burst size were simulated.

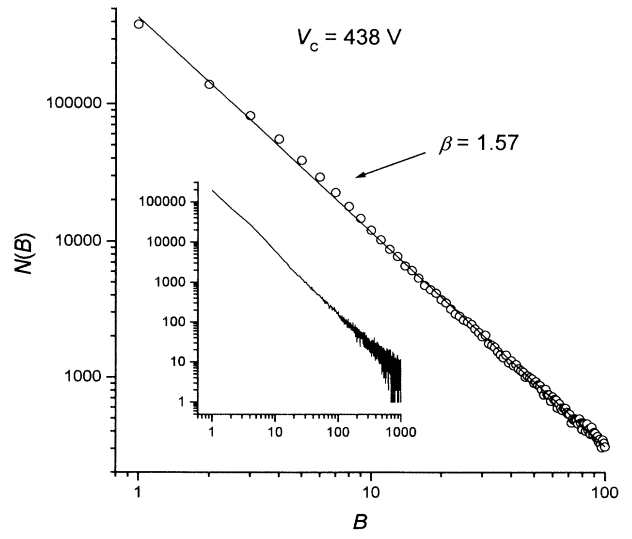

FIG. 6. Burst size distribution $N(B)$ for $p=3$ mbar, $\gamma=0.1$ at the critical voltage $V_c=438$ V for the burst size range $B=1-100$ and the best-fitting power-law function $B^{-\beta}$ with the critical exponent $\beta=1.57$. (The number of simulated bursts is 10^6.) The inset shows the $N(B)$ distribution at the same parameter values, for the burst size range $B=1-1000$, obtained from the simulation of 5×10^5 bursts. $N(B)$ exhibits a self-similar power-law dependence on B over more decades.

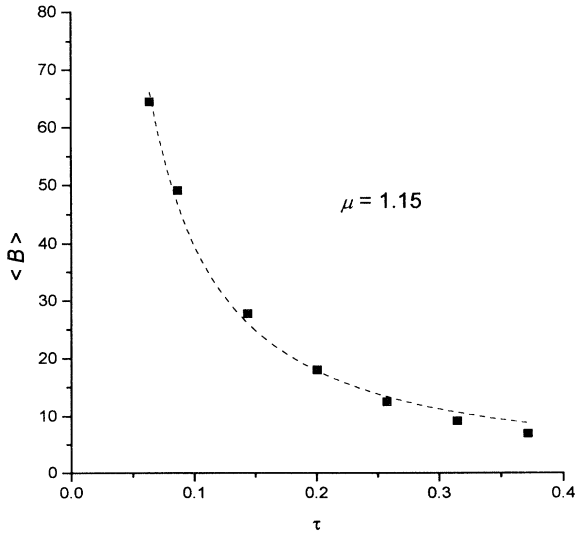

FIG. 8. Average burst size ($\langle B\rangle$) as a function of the parameter $\tau=(V_c-V)/V_c$. The best-fitting critical exponent was found to be $\mu=1.15$. Each data point represents 10^6 simulated bursts.

Once the number of avalanches or the burst size exceeded the predefined limits, the simulation of the given burst was stopped.

The dependence of the average number of avalanches in a burst $\langle A \rangle$ and the average burst size $\langle B \rangle$ on the applied voltage was also studied. These quantities have been calculated as functions of the parameter

$$\tau = \frac{V_c - V}{V_c} . \tag{4}$$

Figures 7 and 8 show our results for $\langle A \rangle$ and $\langle B \rangle$ plotted against τ. The figures also include the best-fitting power-law functions of the form

$$\langle A \rangle \propto \tau^{-\delta} , \tag{5}$$

$$\langle B \rangle \propto \tau^{-\mu} . \tag{6}$$

It can be seen in Figs. 7 and 8 that both the average number of avalanches in a burst and the average total number of electrons participating in a burst (i.e., the average burst size) exhibit a power-law dependence on the parameter τ. It is clear from the model that both $\langle A \rangle$ and $\langle B \rangle$ diverge at the critical voltage, where the avalanches sustain themselves. The best-fitting critical exponents for $\langle A \rangle$ and $\langle B \rangle$ are $\delta = 0.92$ and $\mu = 1.15$. Each data point in Figs. 7 and 8 was obtained from the simulation of 10^6 bursts. The accuracy of the δ and μ exponents (estimated similarly to that of the exponents α and β) was found to be 0.03 for both δ and μ.

IV. CONCLUSIONS

We have investigated the statistical properties of electron avalanches and the sequence of avalanches (bursts) initiated by external particles in a buffer gas subjected to an electric field. The critical voltage of the system (when the average number of positive ions created in an electron avalanche is exactly enough to liberate a secondary electron, which induces a new electron avalanche) was found by calculating the average size of electron avalanches as a function of voltage.

Four parameters of the system were found to exhibit a characteristic power-law dependence. We have shown that the $N(A)$ distribution of the number of avalanches A in a burst and the $N(B)$ distribution of the number of electrons participating in a burst (B) scale as $A^{-\alpha}$ and $B^{-\beta}$, respectively, with $\alpha = 1.58 + 0.02$ and $\beta = 1.57 \pm 0.03$.

The average values of A and B as functions of the parameter $\tau = (V_c - V)/V_c$ were also found to exhibit a power-law dependence $\langle A \rangle \propto \tau^{-\delta}$ and $\langle B \rangle \propto \tau^{-\mu}$ with $\delta = 0.92 \pm 0.03$ and $\mu = 1.15 \pm 0.03$. Our results confirm that at $V = V_c$ the gas discharge system is in a *critical state,* which can be characterized by several nontrivial critical exponents.

ACKNOWLEDGMENTS

This work was supported by a Hungarian Science Foundation Grant No. OTKA-F-7475. I thank Professor P. Szépfalusy, Dr. K. Rózsa, Dr. G. Vattay, A. Kőházi-Kis, and L. Szalai for useful discussions on the subject of this work.

[1] P. Bak, C. Tang, and K. Wiesenfeld, Phys. Rev. A **38**, 364 (1988).
[2] L. P. Kadanoff, S. R. Nagel, L. Wu, and S. Zhou, Phys. Rev. A **39**, 6524 (1989).
[3] Z. Cheng, S. Redner, P. Meakin, and F. Family, Phys. Rev. A **40**, 5922 (1989).
[4] K. L. Babcock and R. M. Westervelt, Phys. Rev. Lett. **64**, 2168 (1990).
[5] G. F. Knoll, *Radiation Detection and Measurement* (Wiley, New York, 1979).
[6] J. M. Meek and J. D. Craggs, *Electrical Breakdown of Gases* (Clarendon, Oxford, 1953).
[7] P. F. Little, in *Encyclopaedia of Physics,* edited by S. Flügge (Springer, Berlin, 1956), Vol. XXI, p. 573.
[8] W. B. Maier, A. Kadish, C. J. Buchenauer, and R. T. Robiscoe, IEEE Trans. Plasma Sci. **21**, 676 (1993).
[9] P. Osmokrović, IEEE Trans. Plasma Sci. **21**, 645 (1993).
[10] A. V. Eletskii and B. M. Smirnov, J. Phys. D **24**, 2175 (1991).
[11] A. V. Kozyrev, Yu D. Korolev, V. G. Rabotkin, and I. A. Shemyakin, J. Appl. Phys. **74**, 5366 (1993).
[12] C. Schultheiss, K. Mittag, D. Dietrich, and W. Bauer, Nucl. Instrum. Methods Phys. Res. Sect. A **294**, 411 (1990).
[13] A. D. Ernest, S. C. Haydon, and Wang Yumin, J. Phys. D **25**, 1187 (1992).
[14] M. J. Noy and A. D. Ernest, J. Phys. D **25**, 1210 (1992).
[15] Tran Ngoc An, E. Marode, and P. C. Johnson, J. Phys. D **10**, 2317 (1977).
[16] J. P. Boeuf and E. Marode, J. Phys. D **15**, 2169 (1982).
[17] E. Marode and J. P. Boeuf, in *Proceedings of the XVI International Conference on Phenomena in Ionized Gases, Düsseldorf, Invited Papers,* edited by W. Bötticher, H. Wenk, and E. Schulz-Gulde (University of Düsseldorf, Düsseldorf, 1983), p. 206.
[18] R. J. Carman, J. Phys. D **22**, 55 (1989).
[19] E. A. Den Hartog, D. A. Doughty, and J. E. Lawler, Phys. Rev. A **38**, 2471 (1988).
[20] F. J. de Heer and R. H. J. Jansen, J. Phys. B **10**, 3741 (1977).
[21] F. J. de Heer, R. H. J. Jansen, and W. van der Kaay, J. Phys. B **12**, 979 (1979).
[22] L. N. Labahn and J. Callaway, Phys. Rev. A **2**, 366 (1970).